Outage Probability of an AF Full-Duplex Physical-Layer Network Coding System

Bilal A. Jebur, Charalampos C. Tsimenidis, Martin Johnston, Jonathon Chambers
School of Electrical and Electronic Engineering, Newcastle University
Newcastle upon Tyne, NE1 7RU, UK
Email: {b.a.jebur, Charalampos.Tsimenidis, Martin.Johnston, Jonathon.Chambers}@newcastle.ac.uk

***Abstract*—In this paper, we investigate the performance of a full-duplex (FD) physical-layer network coding (FD-PLNC) scheme using amplify-and-forward (AF) relaying and orthogonal frequency-division multiplexing (OFDM) for a two-way relay channel (TWRC) network over reciprocal, asymmetric, and frequency-selective Rayleigh fading channels. Furthermore, the proposed system is integrated with a self-interference cancellation (SIC) scheme to effectively reduce the self-interference (SI). Moreover, the impact of the residual SI on the performance of the proposed AF-FD-PLNC is examined. Closed-form expressions for the distribution of the end-to-end (E2E) signal to interference and noise ratio (SINR) and the outage probability are derived and presented. Furthermore, the analytical outage probability results are validated by simulation studies. The results confirm the feasibility of the proposed AF-FD-PLNC and its capability to double the throughput of conventional amplify-and-forward half-duplex physical-layer network coding (AF-HD-PLNC).**

***Index Terms*—Full-duplex physical-layer network coding (FD-PLNC), orthogonal frequency-division multiplexing (OFDM), amplify-and-forward (AF), self-interference cancellation (SIC), amplify-and-forward half-duplex physical-layer network coding (AF-HD-PLNC)**

I. Introduction

Recently, physical-layer network coding (PLNC) systems have been the center of research interest due to their ability to improve the throughput of a two-way relay channel (TWRC) network [1]. A PLNC system consists of two end nodes, denoted A and B, which communicate with the assistance of one relay node R. In this paper, we consider the amplify-and-forward (AF) PLNC relaying scheme, whose transmission schedule comprises two phases, i.e. multiple access (MA) phase and broadcast (BC) phase. During the MA phase, the end nodes transmit their data concurrently to the relay; in contrast, during the BC phase the relay broadcasts a scaled version of the signal received in the MA phase [2].

A. Related Work

The self-interference (SI) signal in full-duplex (FD) systems can dramatically degrade end-to-end (E2E) performance. Consequently, most previous research considers half-duplex (HD) PLNC to avoid SI induced performance degradation. However, recently self-interference cancellation (SIC) schemes have been investigated in [3] and [4] demonstrating the feasibility of implementing pragmatic FD wireless systems. Thus, currently, some researchers have been working on FD cooperative systems. In [5], the feasibility of FD one-way relaying was studied in the presence of loop interference. The diversity and error performances of the FD one-way AF relay channel system, where the HD source node transmits information to the HD destination node with the help of one FD relay node, were studied under the effect of residual SI in [6]. Furthermore, we introduced an orthogonal frequency-division multiplexing (OFDM) based denoise-and-forward (DNF) FD-PLNC, where both the end nodes and the relay operate in FD mode, in [7].

B. Contribution

In this paper, we present an AF-FD-PLNC approach using OFDM. Moreover, in order to minimize the SI, the proposed system is integrated with an SIC scheme. Furthermore, the performance of the proposed system is investigated under the effect of residual SI. The main contributions of this work are as follows:

- We investigate the performance of the proposed system in reciprocal, asymmetric, and frequency-selective Rayleigh fading channels.
- A closed-form expression for the end-to-end (E2E) probability density function (PDF) of the signal to interference and noise ratio (SINR) is derived.
- An E2E outage probability expression for the proposed AF-FD-PLNC is derived and is validated by simulation based E2E outage probability results.

C. Paper Organization

The remainder of the paper is organized as follows: The system model is described in Section II. Section III presents the derivation of the SINR. Section IV shows the derivation of the E2E probability density function (PDF) and the E2E outage probability. The analytical and simulation based results of the proposed system are presented in Section V. Finally, the conclusions of this paper are presented in Section VI.

II. System Model

We consider a FD-TWRC employing uncoded M-ary phase shift keying (MPSK), where two FD end nodes, denoted A and B, with no direct path connecting them, exploit the assistance of one FD relay node, R, to exchange information using the AF relaying scheme. Furthermore, each node in the proposed system is equipped only with two antennas dedicated for transmission and reception, respectively, as depicted in Fig. 1. It can be observed from Fig. 1 that the proposed system

The authors are with the School of Electrical and Electronic Engineering, Newcastle University, England, United Kingdom. In addition, Bilal A. Jebur is also a staff member with the University of Mosul, Iraq and sponsored for PhD study by the MOHESR in Iraq.

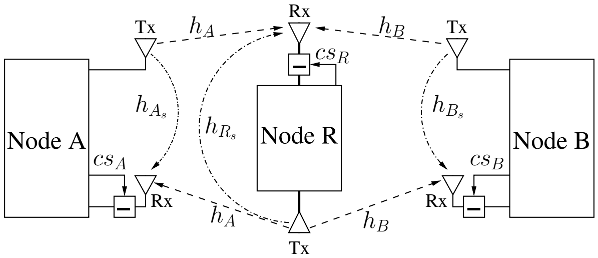

Fig. 1. Full-duplex physical_layer network coding (FD-PLNC) system.

description contains two channel categories. These are the self-interference channels between the TX and RX antennas at each node, and the channels between the nodes, which are considered to be quasi-static asymmetric and reciprocal frequency-selective Rayleigh fading channels. Therefore, the OFDM scheme is exploited to overcome the intersymbol interference (ISI) introduced by these frequency-selective channels. The length of the cyclic-prefix (CP), L_{CP}, in the utilized OFDM scheme is chosen so that $L_{CP} \geqslant \max\{L_A, L_B, L_{J_s}\}$, where, L_A and L_B denote the maximum delay spreads of the channels between the end nodes, A and B, and the relay node; and $L_{J_s} \in \{L_{A_s}, L_{B_s}, L_{R_s}\}$, represents the set of maximum delay spreads of the self-interference channels at each node.

Since all the nodes in the proposed AF-FD-PLNC system transmit and receive simultaneously, the received signal at each node contains SI. Subsequently, the received signal at the relay node after removing the CP and performing an FFT is given as

$$\begin{aligned} Y_R(t,u) = &X_A(t,u)H_A(u) + X_B(t,u)H_B(u) \\ &+ X_R(t,u)H_{R_s}(u) + N_R(u), \end{aligned} \tag{1}$$

while the received signal at the end nodes is given as

$$Y_D(t,u) = X_R(t,u)H_D(u) + X_D(t,u)H_{D_s}(u) + N_D(u), \tag{2}$$

where $D \in \{A, B\}$ whilst $D_s \in \{A_s, B_s\}$, X_A, X_B and X_R represent the signals transmitted by the nodes A, B and R, respectively. N_R and N_D denote the additive white Gaussian noise (AWGN) samples at each node, which follow a complex-valued circular Gaussian distribution, whose PDFs are $\mathcal{CN}(0, N_0^R)$ and $\mathcal{CN}(0, N_0^D)$, respectively. Moreover, H_A and H_B are the frequency responses of the reciprocal channels between the relay and the end nodes, i.e. A and B, respectively, while H_{A_s}, H_{B_s} and H_{R_s} represent the frequency response of the self-interference channels at each node. Finally, $t = 1, 2, \ldots, T$ and $u = 1, 2, \ldots, U$ denote the time slot and subcarrier indices, respectively.

The signals transmitted by the end nodes, X_A and X_B, are obtained by modulating the given data using MPSK modulation. On the other hand, since the AF relaying scheme is exploited at the relay, the transmitted signal from the relay node, i.e. X_R, is obtained by scaling the received superimposed signal from the end nodes during the previous time slot by a factor, F. This scaling factor is given as

$$F(t,u) = \sqrt{\frac{E_{b_R}}{E_{b_A}|H_A(u)|^2 + E_{b_B}|H_B(u)|^2 + \sigma^2_{SI_R} E_{b_R} + N_0^R}}, \tag{3}$$

where E_{b_A}, E_{b_B} and E_{b_R}, are the average bit energies for the signals transmitted from nodes A, B and R, respectively. Therefore, the end nodes' received signal can be rewritten as

$$\begin{aligned} Y_D(t,u) = &F(t,u)Y_R(t-1,u)H_D(u) + X_D(t,u)H_{D_s}(u) \\ &+ N_D(u). \end{aligned} \tag{4}$$

A maximum-likelihood (ML) detector is used at each end node in order to extract the data transmitted by the other end node from the received signal. This ML detector exploits the nodes knowledge of its own transmitted signal during the previous time slot to estimate the signal transmitted from the other end node in the previous time slot as follows

$$\begin{aligned} \hat{X}_A(t-1,u) = &\underset{(q)\in\mathbb{Z}_M}{\text{argmin}} \mid Y_B(t,u) - F(t,u)H_B(u) \\ &\times (H_A(u)\mathcal{C}(q)) + H_B(u)X_B(t-1,u)) \mid^2, \end{aligned} \tag{5}$$

$$\begin{aligned} \hat{X}_B(t-1,u) = &\underset{(q)\in\mathbb{Z}_M}{\text{argmin}} \mid Y_A(t,u) - F(t,u)H_A(u) \\ &\times (H_A(u)X_A(t-1,u) + H_B(u)\mathcal{C}(q)) \mid^2, \end{aligned} \tag{6}$$

where $\mathcal{C}$ represents the MPSK constellation vector.

It is axiomatic that the throughput of FD systems is double the throughput of HD systems. Yet this cannot be achieved unless the SI signal is effectively suppressed. Therefore, each node in the proposed AF-FD-PLNC is integrated with an SIC scheme to minimize the effect of the SI. This SIC scheme uses the perfect knowledge of the node's transmitted signal and the estimated version of the self-interference channel to generate a cancelling signal (CS), which is given in the frequency domain as

$$CS_J(t,u) = \hat{H}_{J_s}(u)X_J(t,u), \tag{7}$$

where $\hat{H}_{J_s}$ is the estimated version of the self-interference channel, H_{J_s}, $J_s \in \{A_s, B_s, R_s\}$ and $J \in \{A, B, R\}$. Subsequently, CS is subtracted from the received signal to remove the SI signal before the analog-to-digital converter (ADC) to prevent the saturation of the ADC. As a result, the received signal at the relay after the SIC is given as

$$\begin{aligned} \tilde{Y}_R(t,u) = &\left(H_{R_s}(u) - \hat{H}_{R_s}(u)\right) X_R(t,u) + X_A(t,u)H_A(u) \\ &+ X_B(t,u)H_B(u) + N_R(u), \end{aligned} \tag{8}$$

while the received signal at the end nodes after the SIC is given as

$$\begin{aligned} \tilde{Y}_D(t,u) = &\left(H_{D_s}(u) - \hat{H}_{D_s}(u)\right) X_D(t,u) \\ &+ F(t,u)\tilde{Y}_R(t-1,u)H_D(u) + N_D(u). \end{aligned} \tag{9}$$

A closer inspection of (8) and (9) reveals that the SI signal could be removed entirely if perfect channel state information (CSI) for $\hat{H}_{R_s}$ and $\hat{H}_{Ds}$ was available. However, due to the channel estimation limitations perfect SIC cannot be attained. Perfect CSI is usually expressed as

$$H_{J_s} = \hat{H}_{J_s} + \xi_{J_s}, \tag{10}$$

where ξ_{J_s} is the channel estimation error modelled as a circular complex Gaussian distribution, i.e. $\mathcal{CN}(0, \sigma^2_{\xi_{J_s}})$ and results from AWGN and other channel disturbances. However, this channel estimation error is expected to be very small as the power of the AWGN and this channel disturbances is generally much smaller than the power of the SI. Hence, the residual SI will typically be rather small.

Using (10) to substitute H_{R_s} and H_{D_s} in (8) and (9), respectively, and after straightforward mathematical simplifications the received signal at the relay after the SIC is given as

$$\begin{aligned}\tilde{Y}_R(t,u) = SI_R(u)X_R(t,u) + X_A(t,u)H_A(u)\\ + X_B(t,u)H_B(u) + N_R(u),\end{aligned} \tag{11}$$

while the received signal at the end nodes after the SIC is given as

$$\begin{aligned}\tilde{Y}_D(t,u) =& F(t,u)\tilde{Y}_R(t-1,u)H_D(u) + SI_D(u)X_D(t,u)\\ &+ N_D(u),\end{aligned} \tag{12}$$

where $SI_J(u)X_J(t,u)$ denotes the residual SI and SI_J exhibits a circular complex Gaussian distribution, i.e. $\mathcal{CN}(0,\sigma^2_{SI_J})$, for $J \in \{A,B,R\}$.

III. SIGNAL TO INTERFERENCE AND NOISE RATIO (SINR)

It can be observed from (12) that the first term is the term of interest and the rest are considered to be interference and noise terms. Therefore, the E2E SINR can be expressed as

$$\gamma_{E2E} = \frac{\gamma_R\gamma_D}{\gamma_R+\gamma_D+1}, \tag{13}$$

where γ_R is the SINR at the relay node and is given as

$$\gamma_R = \frac{\delta_R(|H_A|^2+|H_B|^2)}{\delta_{IR}+1}, \tag{14}$$

while, γ_D represent the SINR at the end nodes and can be expressed as

$$\gamma_D = \frac{\delta_D|H_D|^2}{\delta_{ID}+1}. \tag{15}$$

Furthermore, $\delta_R = \frac{E_{b_D}}{N_0^R}$ and $\delta_D = \frac{E_{b_R}}{N_0^D}$, represent the signal to noise ratio (SNR) at the relay and end nodes, respectively, whilst δ_{I_R} and δ_{I_D}, are the interference to noise ratio (INR) at the relay and end nodes, respectively, which are given as $\delta_{I_R} = \frac{\sigma^2_{SI_R}E_{b_R}}{N_0^R}$, $\delta_{I_D} = \frac{\sigma^2_{SI_D}E_{b_D}}{N_0^D}$.

IV. OUTAGE PROBABILITY

The cumulative distribution function (CDF) of the E2E SINR for the AF-FD-PLNC can be evaluated using the tight lower bound results of [8] as

$$P_{\gamma_{E2E}}(\gamma) = P_{\gamma_R}(\gamma) + P_{\gamma_D}(\gamma) - P_{\gamma_R}(\gamma)P_{\gamma_D}(\gamma), \tag{16}$$

where $P_{\gamma_R}(\gamma)$ and $P_{\gamma_D}(\gamma)$ are the CDF of the SINR at the relay and the end nodes, respectively. Subsequently, the probability density function (PDF) of the E2E SINR can be given as

$$\begin{aligned}p_{\gamma_{E2E}}(\gamma) =& p_{\gamma_R}(\gamma) + p_{\gamma_D}(\gamma) - \big[p_{\gamma_R}(\gamma)P_{\gamma_D}(\gamma)\\ &+ p_{\gamma_D}(\gamma)P_{\gamma_R}(\gamma)\big],\end{aligned} \tag{17}$$

where $p_{\gamma_R}(\gamma)$ and $p_{\gamma_D}(\gamma)$ denote the PDF of the SINR at the relay and the end nodes, respectively. It is clear that (14) and (15) can be expressed as a combination of two random variables. Thus, the SINR at the end nodes can be expressed as

$$\gamma_R = \frac{\upsilon_R}{\chi_R+1}, \tag{18}$$

and the SINR at the end nodes can be given as

$$\gamma_D = \frac{\upsilon_D}{\chi_D+1}, \tag{19}$$

where $\upsilon_R = \delta_R\left(|H_A|^2+|H_B|^2\right)$ and $\upsilon_D = \delta_D|H_D|^2$ are the SNR terms at the relay and end nodes, respectively, while $\chi_R = \delta_{IR}$ and $\chi_D = \delta_{ID}$ denote the INR terms at the relay and the end nodes, respectively.

Due to the fact that all the channels are Rayleigh fading, the PDF of υ_J and χ_J are given as

$$p_{\upsilon_R}(\upsilon_R) = \frac{\upsilon_R}{{\eta_R}^2}e^{-\frac{\upsilon_R}{\eta_R}}, \tag{20}$$

$$p_{\upsilon_D}(\upsilon_D) = \frac{1}{\eta_D}e^{-\frac{\upsilon_D}{\eta_D}}, \tag{21}$$

$$p_{\chi_J}(\chi_J) = \frac{1}{\vartheta_J}e^{-\frac{\chi_J}{\vartheta_J}}, \tag{22}$$

where $\eta_R = \frac{1}{2}E\{\upsilon_R\}$, $\eta_D = E\{\upsilon_D\}$ and $\vartheta_J = E\{\chi_J\}$. Since the SINR expression comprises the ratio of two random variables, i.e. υ_J and χ_J, the PDF of the SINR can be evaluated using the integral [9, Eq. (4.6)], and therefore the PDF of the SINR is given as

$$p_{\gamma_J}(\gamma) = \int_0^\infty (1+\chi_J)p_{\upsilon_J}\big((1+\chi_J)\gamma\big)p_{\chi_J}(\chi_J)d\chi_J. \tag{23}$$

The PDF of the SINR at the relay can be obtained by using (20) and (22) to substitute $p_{\upsilon_J}(\upsilon_J)$ and $p_{\chi_J}(\chi_J)$ in (23), which results in

$$p_{\gamma_R}(\gamma) = \frac{\gamma e^{-\frac{\gamma}{\eta_R}}}{{\eta_R}^2\vartheta_R}\int_0^\infty (1+\chi_R)^2 e^{-\frac{\gamma\vartheta_R+\eta_R}{\eta_R\vartheta_R}\chi_R}d\chi_R. \tag{24}$$

This integral can be solved using $\int_{x=0}^\infty x^n e^{-\mu x}dx = n!\mu^{-n-1}$ for $[\mathbf{Re}\ \mu > 0]$ [10, Eq. (3.351.3)] to give

$$\begin{aligned}p_{\gamma_R}(\gamma) =& \frac{\gamma e^{-\frac{\gamma}{\eta_R}}}{\eta_R^2\vartheta_R}\left[\frac{\eta_R\vartheta_R}{\gamma\vartheta_R+\eta_R} + 2\left(\frac{\eta_R\vartheta_R}{\gamma\vartheta_R+\eta_R}\right)^2\right.\\ &\left.+ 2\left(\frac{\eta_R\vartheta_R}{\gamma\vartheta_R+\eta_R}\right)^3\right].\end{aligned} \tag{25}$$

Moreover, (21) and (22) are used to substitute $p_{\upsilon_J}(\upsilon_J)$ and $p_{\chi_J}(\chi_J)$ in (23) to evaluate the PDF of the SINR at the end nodes, which is given as

$$p_{\gamma_D}(\gamma) = \frac{e^{-\frac{\gamma}{\eta_D}}}{\eta_D\vartheta_D}\int_0^\infty (1+\chi_D)e^{-\frac{\gamma\vartheta_D+\eta_D}{\eta_D\vartheta_D}\chi_D}d\chi_D. \tag{26}$$

This integral can be evaluated using $\int_{x=0}^\infty x^n e^{-\mu x}dx = n!\mu^{-n-1}$ for $[\mathbf{Re}\ \mu > 0]$ [10, Eq. (3.351.3)]. As a result, the PDF of the SINR at the end nodes is given as

$$p_{\gamma_D}(\gamma) = \frac{e^{-\frac{\gamma}{\eta_D}}}{\eta_D\vartheta_D}\left[\frac{\eta_D\vartheta_D}{\gamma\vartheta_D+\eta_D} + \left(\frac{\eta_D\vartheta_D}{\gamma\vartheta_D+\eta_D}\right)^2\right]. \tag{27}$$

On the other hand, the CDF of the SINR can be computed using [9, Eq. (4.5)] as

$$P_{\gamma_J}(\gamma) = \int_0^\infty P_{\upsilon_J}\big((1+\chi_J)\gamma\big) p_{\chi_J}(\chi_J) d\chi_J, \quad (28)$$

where, the CDF of υ_R, i.e. $P_{\upsilon_R}(\upsilon_J)$, is given as

$$P_{\upsilon_R}(\upsilon_R) = 1 - e^{-\frac{\upsilon_R}{\eta_R}}\left(1 + \frac{\upsilon_R}{\eta_R}\right). \quad (29)$$

Furthermore, the CDF of υ_D is expressed as

$$P_{\upsilon_D}(\upsilon_D) = 1 - e^{-\frac{\upsilon_D}{\eta_D}}. \quad (30)$$

Hence, the CDF of the SINR at the relay can be obtained by using (29) and (22) to substitute $P_{\upsilon_J}(\upsilon_J)$ and $p_{\chi_J}(\chi_J)$ in (28), which results in

$$\begin{aligned} P_{\gamma_R}(\gamma) = & \int_0^\infty \frac{1}{\vartheta_R} e^{-\frac{\chi_R}{\vartheta_R}} d\chi_R - \frac{e^{-\frac{\gamma}{\eta_R}}}{\vartheta_R}\int_0^\infty e^{-\frac{\eta_R+\gamma\vartheta_R}{\eta_R\vartheta_R}\chi_R} d\chi_R \\ & - \frac{\gamma e^{-\frac{\gamma}{\eta_R}}}{\eta_R\vartheta_R}\int_0^\infty e^{-\frac{\eta_R+\gamma\vartheta_R}{\eta_R\vartheta_R}\chi_R} d\chi_R - \frac{\gamma e^{-\frac{\gamma}{\eta_R}}}{\eta_R\vartheta_R} \\ & \times \int_0^\infty \chi_R e^{-\frac{\eta_R+\gamma\vartheta_R}{\eta_R\vartheta_R}\chi_R} d\chi_R. \end{aligned} \quad (31)$$

These integrals can be solved using [10, Eq. (3.351.3)]. Therefore, the CDF of the SINR at the relay is given as

$$P_{\gamma_R}(\gamma) = 1 - \frac{\eta_R e^{-\frac{\gamma}{\eta_R}}}{\eta_R + \gamma\vartheta_R} - \frac{\gamma e^{-\frac{\gamma}{\eta_R}}}{\eta_R + \gamma\vartheta_R} - \frac{\gamma\eta_R\vartheta_R e^{-\frac{\gamma}{\eta_R}}}{(\eta_R + \gamma\vartheta_R)^2}. \quad (32)$$

Furthermore, the CDF of the SINR at the end nodes can be evaluated by using (30) and (22) to substitute $P_{\upsilon_J}(\upsilon_J)$ and $p_{\chi_J}(\chi_J)$ in (28), which yields

$$P_{\gamma_D}(\gamma) = \int_0^\infty \frac{1}{\vartheta_D} e^{-\frac{\chi_D}{\vartheta_D}} d\chi_D - \frac{e^{-\frac{\gamma}{\eta_D}}}{\vartheta_D}\int_0^\infty e^{-\frac{\eta_D+\gamma\vartheta_D}{\eta_D\vartheta_D}\chi_D} d\chi_D. \quad (33)$$

Solving these integrals yields the CDF of the SINR at the end nodes, which is given as

$$P_{\gamma_D}(\gamma) = 1 - \frac{\eta_D e^{-\frac{\gamma}{\eta_D}}}{\gamma\vartheta_D + \eta_D}. \quad (34)$$

The PDF of the E2E SINR can be evaluated by using (25), (27), (32) and (34) to substitute $p_{\gamma_R}(\gamma)$, $p_{\gamma_D}(\gamma)$, $P_{\gamma_R}(\gamma)$ and $P_{\gamma_R}(\gamma)$ in (17), respectively, which results in

$$\begin{aligned} p_{\gamma_{E2E}}(\gamma) = & \frac{\gamma\eta_D e^{-\frac{\eta_R+\eta_D}{\eta_R\eta_D}\gamma}}{\eta_R{}^2\vartheta_R(\gamma\vartheta_D + \eta_D)}\left[\frac{\eta_R\vartheta_R}{\gamma\vartheta_R + \eta_R}\right. \\ & \left. + 2\left(\frac{\eta_R\vartheta_R}{\gamma\vartheta_R + \eta_R}\right)^2 + 2\left(\frac{\eta_R\vartheta_R}{\gamma\vartheta_R + \eta_R}\right)^3\right] \\ & + \frac{e^{-\frac{\eta_R+\eta_D}{\eta_R\eta_D}\gamma}}{\eta_D\vartheta_D}\left[\frac{\eta_D\vartheta_D}{\gamma\vartheta_D + \eta_D} + \left(\frac{\eta_D\vartheta_D}{\gamma\vartheta_D + \eta_D}\right)^2\right] \\ & \times \left[\frac{\eta_R}{\eta_R + \gamma\vartheta_R} + \frac{\gamma}{\eta_R + \gamma\vartheta_R} + \frac{\gamma\eta_R\vartheta_R}{(\eta_R + \gamma\vartheta_R)^2}\right]. \end{aligned} \quad (35)$$

Furthermore, the CDF of the E2E SINR can be computed by using (32) and (34) to substitute $P_{\gamma_R}(\gamma)$ and $P_{\gamma_R}(\gamma)$ in (16), respectively, which yields

$$\begin{aligned} P_{\gamma_{E2E}}(\gamma) = 1 - & \frac{e^{-\frac{\eta_R+\eta_D}{\eta_R\eta_D}\gamma}\eta_D}{\gamma\vartheta_D + \eta_D}\left[\frac{\eta_R}{\eta_R + \gamma\vartheta_R} + \frac{\gamma}{\eta_R + \gamma\vartheta_R}\right. \\ & \left. + \frac{\gamma\eta_R\vartheta_R}{(\eta_R + \gamma\vartheta_R)^2}\right]. \end{aligned} \quad (36)$$

The outage probability is obtained by computing the probability that the SINR falls below a specific threshold, γ_{th} [11]. Thus, the E2E outage probability is given as

$$\begin{aligned} P_{out}^{E2E}(\gamma_{E2E_{th}}) & \triangleq Pr\{\gamma_{E2E} \leq \gamma_{E2E_{th}}\} \\ & = \int_0^{\gamma_{E2E_{th}}} p_{\gamma_{E2E}}(\gamma) d\gamma. \end{aligned} \quad (37)$$

The E2E outage probability can also be expressed as

$$P_{out}^{E2E}(\gamma_{E2E_{th}}) = P_{\gamma_{E2E}}(\gamma_{E2E_{th}}). \quad (38)$$

Therefore, the E2E outage probability is given as

$$\begin{aligned} P_{out}^{E2E}(\gamma_{E2E_{th}}) = 1 - & \frac{e^{-\frac{\eta_R+\eta_D}{\eta_R\eta_D}\gamma_{E2E_{th}}}\eta_D}{\gamma_{E2E_{th}}\vartheta_D + \eta_D}\left[\frac{\eta_R}{\eta_R + \gamma_{E2E_{th}}\vartheta_R}\right. \\ & \left. + \frac{\gamma_{E2E_{th}}}{\eta_R + \gamma_{E2E_{th}}\vartheta_R} + \frac{\gamma_{E2E_{th}}\eta_R\vartheta_R}{(\eta_R + \gamma_{E2E_{th}}\vartheta_R)^2}\right]. \end{aligned} \quad (39)$$

On the other hand, the AF-HD-PLNC system is SI free. Hence, the CDF of the SNR at the relay is given as

$$P_{\gamma_R^{HD}}(\gamma^{HD}) = 1 - e^{-\frac{\gamma^{HD}}{\eta_R^{HD}}}\left(1 + \frac{\gamma^{HD}}{\eta_R^{HD}}\right), \quad (40)$$

whilst the CDF of the SNR at the end nodes is given as

$$P_{\gamma_D^{HD}}(\gamma^{HD}) = 1 - e^{-\frac{\gamma^{HD}}{\eta_D^{HD}}}. \quad (41)$$

As a result, the outage probability of the AF-HD-PLNC can be evaluated using (40) and (41) to substitute $P_{\gamma_R}(\gamma)$ and $P_{\gamma_D}(\gamma)$ in (16), which results in

$$P_{out}^{HD_{E2E}}(\gamma_{E2E_{th}}^{HD}) = 1 - e^{-\frac{(\eta_R^{HD}+\eta_D^{HD})\gamma_{E2E_{th}}^{HD}}{\eta_R^{HD}\eta_D^{HD}}}\left(1 + \frac{\gamma_{E2E_{th}}^{HD}}{\eta_R^{HD}}\right). \quad (42)$$

V. Numerical Results

This section presents the analytical and the simulation based results for the proposed OFDM based AD-FD-PLNC. We consider FD-TWRC network scheme utilizing uncoded quadrature phase shift keying (QPSK), where two end nodes exchange information with the aid of an AF relay node over asymmetric frequency selective Rayleigh fading channels. The utilized OFDM system parameters are given in Table I, while the average channel impulse responses utilized in the simulations are given in Table II and III.

TABLE I
SIMULATION SETTING.

Packet length	4096 (bit)
Number of subcarriers	2048
Length of cyclic prefix (CP)	128
Total Number of transmitted bits	409600000
Constellation vector	$\mathcal{C} \in \{\pm 1 \pm j\}$

First, the analytical E2E SINR distribution of the AF-FD-PLNC was derived and computed as depicted in Fig. 2 demonstrating the impact of the residual SI on the distribution of the E2E SINR. It is noticeable from Fig. 2 that the PDF of

TABLE II
CHANNEL MODEL OF THE CHANNEL BETWEEN NODE A AND THE RELAY.

Delay (ns)	0	105	186	426
Average Power (dB)	0.0	-10.5	-18.0	-21.3

TABLE III
CHANNEL MODEL OF THE CHANNEL BETWEEN NODE B AND THE RELAY.

Delay (ns)	0	201	802	1203	2306	3709
Average Power (dB)	0.0	-0.7	-4.8	-8.1	-7.7	-23.8

the E2E SINR converges in the low SINR area as the amount of the residual SI increases. Second, in order to investigate the feasibility of the proposed AF-FD-PLNC in the presence of the residual SI, the E2E outage probability expression is derived and presented. Furthermore, the analytical outage probability results of the AF-FD-PLNC were validated by simulation based results and compared with those of the AF-HD-PLNC as shown in Fig. 3.

Fig. 3 depicts the analytical and simulation based outage probability results for the conventional AF-HD-PLNC and the proposed AF-FD-PLNC with three different scenarios of residual SI to noise ratio, namely $\delta_{IR} = \delta_{IA} = \delta_{IB} = 0,\ 5,\ 10$ dB, respectively, vs. SNR after the SIC, whilst the SINR threshold, γ_{th}, was fixed at 15 dB. Comparing the outage probability results of the AF-HD-PLNC with the results of the AF-FD-PLNC reveals that there is a penalty in SNR of 3.1, 6.3 and 10.5 dB, respectively, when the residual SI to noise ratio at each node ranges from 0 to 10 dB.

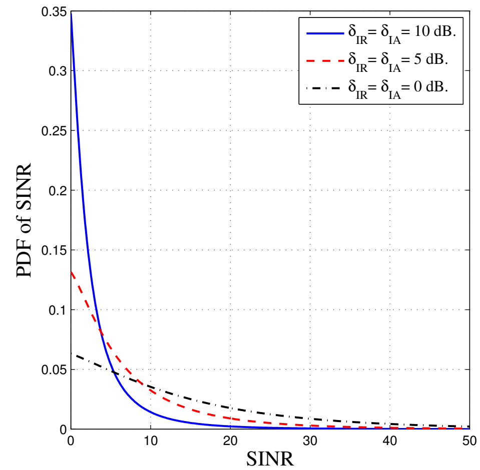

Fig. 2. The PDF of the SINR at node A after the active SIC for DNF-FD-PLNC with different levels of residual SI at SNR δ_A=15 dB.

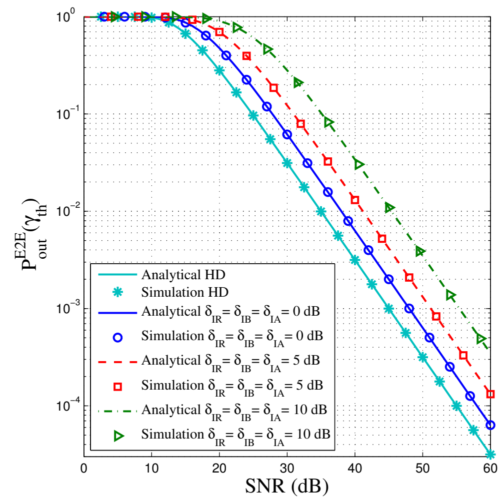

Fig. 3. The analytical and simulation average E2E outage probability for AF-HD-PLNC and AF-FD-PLNC after the active SIC at $\gamma_{E2E_{th}}$=15 dB.

VI. CONCLUSIONS

In this paper the performance of the proposed OFDM based AF-FD-PLNC over asymmetric frequency-selective Rayleigh fading channels was studied and analyzed under the effect of residual SI. Moreover, the proposed AF-FD-PLNC was integrated with an active SIC scheme to effectively mitigate the effect of the SI signal. A closed-from expression for the E2E SINR distribution was derived and presented. This expression was used to compute the analytical distribution after the active SIC. Furthermore, a closed-form expression for the E2E outage probability was presented and validated by simulation based results. The obtained results have confirmed the feasibility of AF-FD-PLNC. Moreover, although the throughput of the proposed AF-FD-PLNC is double the throughput of the conventional AF-HD-PLNC, the comparison between their outage probability results reveals that there is an SNR penalty in the proposed AF-FD-PLNC system, which varies with the amount of the residual SI.

REFERENCES

[1] S. C. Liew, S. Zhang, and L. Lu, "Physical-layer network coding: Tutorial, survey, and beyond," *Physical Communication*, vol. 6, pp. 4–42, 2013.

[2] L. Yang, K. Qaraqe, E. Serpedin, and M.-S. Alouini, "Performance analysis of amplify-and-forward two-way relaying with co-channel interference and channel estimation error," *IEEE Trans. Commun.*, vol. 61, no. 6, pp. 2221–2231, June 2013.

[3] M. Duarte, C. Dick, and A. Sabharwal, "Experiment-driven characterization of full-duplex wireless systems," *IEEE Trans. Wireless Commun.*, vol. 11, no. 12, pp. 4296–4307, December 2012.

[4] E. Ahmed and A. Eltawil, "All-digital self-interference cancellation technique for full-duplex systems," *IEEE Trans. Wireless Commun.*, vol. 14, no. 7, pp. 3519–3532, July 2015.

[5] T. Riihonen, S. Werner, R. Wichman, and Z. Eduardo, "On the feasibility of full-duplex relaying in the presence of loop interference," in *IEEE 10th Workshop on Signal Processing Advances in Wireless Communications (SPAWC)*, June 2009, pp. 275–279.

[6] L. Jimenez Rodriguez, N. Tran, and T. Le-Ngoc, "Performance of full-duplex AF relaying in the presence of residual self-interference," *IEEE J. Sel. Areas Commun.*, vol. 32, no. 9, pp. 1752–1764, Sept 2014.

[7] B. Jebur and C. Tsimenidis, "Performance analysis of OFDM-Based denoise-and-forward full-duplex PLNC with imperfect CSI," in *IEEE International Conference on Communication Workshop (ICCW)*, June 2015, pp. 997–1002.

[8] K. Hemachandra and N. Beaulieu, "Outage analysis of opportunistic scheduling in dual-hop multiuser relay networks in the presence of interference," *IEEE Trans. Commun.*, vol. 61, no. 5, pp. 1786–1796, May 2013.

[9] M. Ahsanullah, B. G. Kibria, and M. Shakil, *Normal and Student's t Distributions and Their Applications*. Springer, 2014.

[10] A. Jeffrey and D. Zwillinger, *Table of integrals, series, and products*. Academic Press, 2007.

[11] M. K. Simon and M.-S. Alouini, *Digital communication over fading channels*. John Wiley & Sons, 2005.